

Latent Plans for Task-Agnostic Offline Reinforcement Learning

Erick Rosete-Beas^{1*}, Oier Mees^{1*}, Gabriel Kalweit¹, Joschka Boedecker¹, Wolfram Burgard²

¹University of Freiburg ²University of Technology Nuremberg

<http://tacorl.cs.uni-freiburg.de>

Abstract: Everyday tasks of long-horizon and comprising a sequence of multiple implicit subtasks still impose a major challenge in offline robot control. While a number of prior methods aimed to address this setting with variants of imitation and offline reinforcement learning, the learned behavior is typically narrow and often struggles to reach configurable long-horizon goals. As both paradigms have complementary strengths and weaknesses, we propose a novel hierarchical approach that combines the strengths of both methods to learn task-agnostic long-horizon policies from high-dimensional camera observations. Concretely, we combine a low-level policy that learns latent skills via imitation learning and a high-level policy learned from offline reinforcement learning for skill-chaining the latent behavior priors. Experiments in various simulated and real robot control tasks show that our formulation enables producing previously unseen combinations of skills to reach temporally extended goals by “stitching” together latent skills through goal chaining with an order-of-magnitude improvement in performance upon state-of-the-art baselines. We even learn one multi-task visuomotor policy for 25 distinct manipulation tasks in the real world which outperforms both imitation learning and offline reinforcement learning techniques.

Keywords: Offline Reinforcement Learning, Imitation Learning, Robot Learning

1 Introduction

In recent years, reinforcement learning (RL) has achieved tremendous successes in a variety of domains [1, 2, 3, 4]. Especially offline RL [5, 6, 7, 8, 9, 10] with its appealing property to estimate (close-to) optimal policies from previously collected and fixed datasets yielded a strong current in robot control research. However, despite the exceptional progress in this fast-moving field, current offline RL methods are often evaluated on highly specific and artificial benchmarks lacking the complexity and long-term dependencies of everyday tasks, which inherently entail a sequential relationship of multiple implicit subtasks. It lies in the nature of such composite tasks that this translates to estimating optimal actions for a significant amount of consecutive decision steps, making learning of such optimal policies very difficult. In fact, Kidambi et al. [11] discovered a quadratic relationship between the horizon of a task and the worst-case accumulated error of any offline RL method. This poses a major challenge especially in case of raw and unstructured sensory inputs, as robots must be capable of learning a large repertoire of skills and combine them to perform everyday tasks acting on long time scales.

One way to alleviate the problem of long horizons is the hierarchical subdivision of a task into high- and low-level policies, where a high-level policy is chaining executions of multiple low-level policies over primitives. Most commonly, such hierarchical structures are rather rigid and act upon a *fixed* number of low-level policies, thus lacking the flexibility and extendability required for most real-life settings. In addition, the *a priori* definition of useful low-level *skills* or their discovery from data is a highly non-trivial task. Related prior work attempted to solve this via a goal-conditioned reformulation [12] of *Conservative Q-learning* [6]. However, it was shown that on short and distinct robot manipulation tasks, self-supervised learning on unlabeled *play* can significantly surpass the performance of individual expert-trained behavioral-cloning policies [13] – which, on the flip-side, can be on par with computationally expensive offline RL methods in such settings [14, 15]. In this work, we thus propose to leverage *play data*, i.e., non-goal-directed collections of trajectories grounded

*Equal Contribution

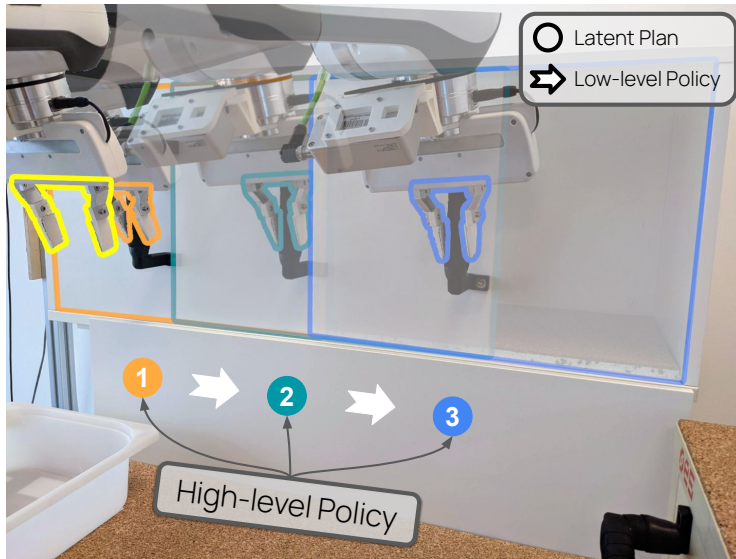


Figure 1. TACO-RL learns a single 7-DoF hierarchical visuomotor policy from offline data. It can solve long-horizon robot manipulation tasks by using a high-level policy that divides a task into a sequence of latent behaviors that are executed by a low-level policy that interacts with the environment. It reduces the effective horizon of the high-level policy and learns to chain skills through dynamic programming.

in human action execution, to estimate *short-horizon* expert policies via *imitation learning* chained via a coarse-grained high-level policy optimized by *offline RL* to account for optimal solutions over *long horizons*. By stitching latent plans extracted from unstructured data, our formulation offers the simplicity of imitation from collected play data while offering long-term optimality for sequential multi-tier tasks. Specifically, we use the collected data to learn our hierarchical policy as acquiring data with good state coverage and visual variety is important for successful applications of offline RL. Play data assumes access to an unsegmented teleoperated dataset of semantically meaningful behaviors provided by users, without a set of predefined tasks in mind. Unlike previous hierarchical approaches, that learn long-horizon tasks by performing a discrete set of tasks with a low-level policy, we are motivated by the idea of an agent capable of task-agnostic control. In this setting, we are endowing the agent with the ability to reach any possible target state from a given initial state. Specifically, we learn a low-level policy that decodes motor control actions from latent skills learned through imitation learning in a self-supervised manner. This low-level policy can perform various behaviors when present in a state by conditioning the policy with a latent plan. Consequently, we also learn a high-level policy that will order these behaviors to achieve long-horizon tasks. This high-level policy is modeled as a goal-conditioned policy that outputs latent plans to be decoded by the low-level policy. The skill-chaining of the behavior priors is learned through offline RL by augmenting plan transitions with hindsight relabeling. This hierarchical approach constitutes a practical solution by decomposing a whole task into smaller chunks of sub-tasks. The high-level policy can learn long-horizon tasks as the effective episode horizon is reduced and it does not need to capture in detail the physics of the world, simplifying the underlying dynamics of the RL agent. The model formulation allows to design a general-purpose training objective by considering every possible state reached in the data as a potential task. Additionally, our approach is effective for learning policies from large and diverse datasets which do not necessarily contain optimal behaviors.

The primary contribution of this work is an hierarchical self-supervised approach to learning task-agnostic control policies from high-dimensional observations by combining model-free RL methods with imitation learning. To our knowledge, our method is the first learning system explicitly aiming to solve long-horizon multi-tier tasks from purely offline and unstructured play data without access to a model. We integrate our components in a unified framework, called Task-AgnostiC Offline Reinforcement Learning (TACO-RL). See Figure 1 for an overview. We show that our model obtains the highest success rate when tested against other state-of-the-art baselines on various long-horizon tasks of the challenging CALVIN environment [16] and that it is able to learn a single visuomotor 7-DoF policy that can perform a wide range of long-horizon manipulation tasks in both a simulated and a real-world tabletop environment. At test time, the real world system is capable of solving a challenging suit of 25 manipulation tasks at 10 Hz that involve more than 300 decisions per task.

2 Related Work

Offline Reinforcement Learning. Offline RL [5], i.e., RL from fixed and possibly mixed transition sets, constitutes a recent trend in RL and robot control research. Generally, at least in model-free

settings, these techniques put a regularization on out-of-distribution actions, so as to enforce the learned policy to remain in the coverage of the dataset, since offline RL methods tend to suffer strongly from the problem of value overestimation. The simplest, yet competitive, attempt to solve this issue is a *behavioral cloning* addendum to a classical actor-critic framework [8]. *Conservative Q-learning* [6], on the other hand, imposes a penalty for actions not covered in the dataset making out-of-distribution actions non-optimal. *Fisher-BRC* parameterizes the critic as the log-behavior-policy [17] extended by a weighted offset term. *Implicit Q-learning* [10] modifies the Bellman optimality update towards a SARSA-like update, maximizing only over actions in the data-set. However, the rationale behind most current offline RL methods remains rather similar. While we make use of *Conservative Q-learning* in our experiments – which recently emerged as one of the most widely used benchmarks in offline RL – we want to point out that any other sophisticated improvement upon the classical offline RL objective is orthogonal to our work and could in principle be incorporated in our framework.

Hierarchical policy learning. Hierarchical policy learning involves learning a hierarchy of policies where a low-level policy performs motor control actions and a high-level policy directs the low-level policy to solve a task. While some works [18, 19, 20] learn a discrete set of low-level policies, each behaving as a primitive skill, this is not appropriate for a general-purpose robot that accomplishes a continuum of behaviors. A large body of hierarchical policy optimization approaches following a similar rationale to our method use planning in latent state spaces [21, 22, 23, 24, 25, 26, 27, 28] and hence require a model covering the complex dynamics of multistep skills, which is an active field of research on its own. We alleviate the necessity of a model by estimating the high-level policy via model-free RL as opposed to model-based planning and thus keep the optimization over the continuous set of skills completely at training time. In contrast to a plethora of prior work [29, 30, 31, 32, 33, 34, 35], our approach acts in the offline paradigm as it yields a lot of appealing properties for learning robot control policies. En route to a skill-chaining policy able to solve long-horizon problems, our approach exploits unstructured play data to estimate the latent skill embeddings as opposed to other work that relies on expert data or predefined skills [36, 37, 38]. Whilst in principle also other latent skill representations could be considered [39, 40, 41, 42, 43], we build upon Play-LMP [13] as it has already shown great performance and robustness in this very setting. Our design choices are directed towards a general-purpose visuomotor agent that has a high zero-shot generalization even for complex long-horizon tasks, a setting more complex than in previous offline methods [13, 44]. In summary, our approach is aiming to solve temporally extended tasks without the necessity of a model or planning from entirely offline, unstructured, unlabeled and suboptimal data. This unique combination of properties thus adds a scalable and extendable optimization method to the toolbox of robot learning.

3 Mathematical Foundation

In this section, we introduce notation and define the problem setting. We model the interaction between an agent and environment and a goal-conditioned policy as a goal-augmented Markov decision process $M = (S, A, p, r, G, p_0, \gamma)$ where S represents the state-observation space, A represents the action space, $p(s'|s, a)$ is a state-transition probability function, $r(s, a, s')$ represents the reward function, $G \subseteq S$ specifies the goal space, $p_0(s)$ is an initial state distribution, and $\gamma \in (0, 1)$ represents the discount factor. We note that the agent does not have access to the true state of the environment, but to visual observations. We learn in an offline manner by assuming to use a large, unlabeled, and undirected fixed dataset $\mathcal{D} = \{(s_1, a_1), (s_2, a_2), \dots, (s_T, a_T)\}$. We then relabel this long temporal state-action stream to produce a dataset of trajectories $D = \{(\tau_i = (s_t, a_t)_{t=0}^k)\}_{i=1}^N$ that can be used to learn both the low-level and high-level policy without access to a model.

4 Offline goal-conditioned RL with TACO-RL

In this section, we elaborate on TACO-RL. Our proposed method considers the bottom-up approach; we start by training a low-level policy and we use it to provide a higher-level action space for a high-level policy that, due to this task division, is ideally facing an easier learning problem. First, we describe our unsupervised objective, which learns a continuous space of latent-conditioned behaviors $\pi_\omega(a|s_c, z)$ from D , where s_c represents the current state. Afterward, we detail how to learn the high-level policy with offline RL by hindsight relabeling sub-trajectories with the aid of the previously learned low-level policy. This reduces our effective task horizon, making it easier to learn long-horizon tasks. Additionally, the low-level policy will predict actions close to the offline data distribution, bringing stability to the whole learning pipeline. See Figure 2 for an overview.

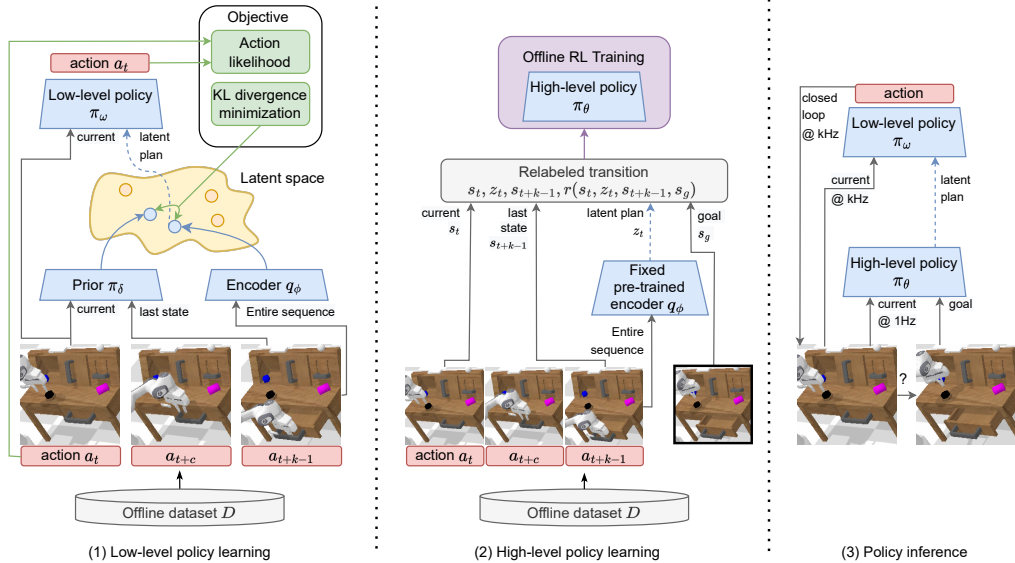


Figure 2. **TACO-RL Overview.** TACO-RL is a self-supervised general-purpose model learned from an offline dataset of robot interactions, it generalizes to a wide variety of long-horizon manipulation tasks. (1) Low-level policy: Recognizes and organizes a repertoire of behaviors from unlabeled, undirected dataset in a latent plan space. (2) High-level policy: Hindsight relabeling of sampled windows of experience into reward-augmented latent plan transitions. Learned with offline RL, this allows the high-level policy to stitch plans together to achieve complex long-horizon tasks. (3) Inference: the hierarchical model is used to perform goal-conditioned rollouts in robot manipulation tasks.

4.1 Learning the low-level policy

We would like to extract a continuous space of primitives that propose meaningful behaviors for an agent to take within a given state. We learn a low-level policy $\pi_\omega(a|s_c, z)$ from the offline, unstructured dataset D that is able to decode a latent plan z to its respective motor-control actions a . After training, we can use the latent plans as an action space for the high-level policy to learn reaching temporally extended goals by “stitching” together latent skills through goal chaining.

In our fixed static dataset D , it is expected to find different valid behaviors achieving the same outcome in a scene, e.g. closing a drawer quickly or slowly. We address this inherent multi-modality by auto-encoding contextual data through a latent plan space with a sequence-to-sequence conditional variational auto-encoder (seq2seq CVAE) [13, 45]. Conditioning the action decoder on the latent plan allows the policy to use the entirety of its capacity for learning uni-modal behavior. Consequently, we propose the following objective for learning the low-level policy $\pi_\omega(a|s_c, z)$:

$$\min_{\omega, \phi} \mathbb{E}_{\tau \sim D, z \sim q_\phi(z|\tau)} \left[- \sum_{t=0}^{|\tau|} \log(\pi_\omega(a_t|s_t, z)) \right], \quad (1)$$

where \mathbb{E} indicates empirical expectation and $q_\phi(z|\tau)$ may be interpreted as the latent plan encoder. As an additional component of the algorithm, we enforce consistency in the latent variables predicted by encoder $q_\phi(z|\tau)$ and prior $\pi_\delta(z|s_t, s_g)$. Since our goal is to obtain a latent plan z that captures a temporal sequence of actions for a given trajectory $\tau = (s_0, a_0, \dots, s_k, a_k)$, we utilize a regularization that enforces the distribution $q_\phi(z|\tau)$ to be close to just predicting the primitive or the latent variable z given the initial and last state of this sub-trajectory, i.e., $\pi_\delta(z|s_c, s_g)$. The Evidence Lower Bound (ELBO) [46] for the CVAE can be written as:

$$\log p(x|s) \geq -\text{KL}(q(z|x, s) \parallel p(z|s)) + \mathbb{E}_{q(z|x, s)} [\log p(x|z, s)]. \quad (2)$$

The conditioning of the prior $\pi_\delta(z|s_c, s_g)$ on the initial and final state regularizes the distribution $q_\phi(z|\tau)$ to not overfit to the complete sub-trajectory τ . In practice, rather than solving the constrained optimization directly, we implement the KL-constraint as a penalty, weighted by an appropriately chosen coefficient β . Thus, one may interpret our objective as using a sequential β -VAE [47]. Finally, we use balancing terms within the KL loss [48, 49], see Appendix D.1.

4.2 Offline RL with Hindsight relabeling

After distilling learned behaviors from D in terms of an encoder $q_\phi(z|\tau)$, a latent behavior policy $\pi_\omega(a|s_c, z)$, and a prior $\pi_\delta(z|s_c, s_g)$, TACO-RL then applies these behaviors to learn a general-purpose agent with offline RL. We formulate a goal augmented MDP by augmenting environment trajectories with a reward function. Thereby, we sample a trajectory from the dataset $\tau \sim D$.

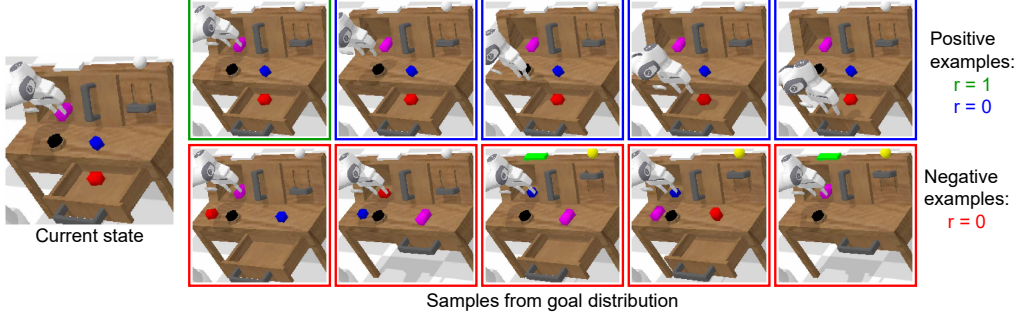


Figure 3. We relabel sampled trajectories into reward augmented transitions by sampling goal states that can be reached after executing a sequence of behaviors. With green border, we have the frame found at the end of the sampled trajectory. As this state will be reached after executing the latent behavior, the reward for this transition is 1. With blue border, we find future states that occur after the sampled sequence. These goals are necessary for chaining behaviors. The reward for these transitions is 0. Finally, with red border, we present images with similar proprioceptive information to the final state in the sampled trajectory, but a different scene arrangement. The reward for these transitions is 0.

Then, we use this trajectory to represent a high-level policy transition by using the pre-trained fixed encoder. For this, we sample a latent plan from the policy encoder $z_t \sim q_\phi(z|\tau)$ and we generate an interaction transition using the sampled latent plan (s_t, z_t, s_{t+k-1}) . To augment this transition with a reward, we use hindsight relabeling with a sparse reward as follows $r(s_t, z_t, s_{t+k-1}, s_g) = \mathbb{1}_{s_{t+k-1}=s_g}$. In this formulation, we assume that during inference we can decode the latent plan using the low-level policy and we will reach the final trajectory state s_{t+k-1} . Note that s_t , s_{t+k-1} , and s_g all represent images, and the reward is only given when the high-level transition reached state and goal state exactly match. During training, goals are sampled according to a distribution $s_g \in \mathcal{S}$, which we will discuss later. Our Q-learning approach corresponds to the following Bellman error optimization objective:

$$\min_{\lambda} \mathbb{E}_{\tau \sim D, z \sim q_\phi(z|\tau), s_g \sim \mathcal{S}} \left[Q_\lambda(s_t, z_t, g) - \hat{Q}(s_t, z_t, g) \right]^2 \quad (3)$$

where: $\hat{Q}(s_t, z_t, g) = \left(\mathbb{1}_{s_{t+k-1}=s_g} + \gamma \mathbb{1}_{s_{t+k-1} \neq s_g} \max_{z_{t+k-1}} Q_\lambda(s_{t+k-1}, z_{t+k-1}, s_g) \right)$

We can then learn a high-level policy $\pi_\theta(z|s_c, s_g)$ with an off-the-shelf offline actor-critic method. In TACO-RL, we use Conservative Q-Learning (CQL) [6] where we initialize the actor weights with the previously learned prior policy $\pi_\delta(z|s_c, s_g)$, as the prior policy is already a good starting point that is able to solve short-horizon tasks.

Selecting goals for relabeling transitions. Our high-level policy is learned via offline RL as we want to learn through dynamic programming how to chain skills to reach long-horizon goals. For this we need to create a formulation that sample goal states s_g that can be reached after executing a sequence of plans. Naively choosing s_g , say by sampling random states uniformly from the dataset, will provide an extremely sparse reward signal, as two random state images will rarely be identical. The sparse reward problem can be mitigated by selectively sampling as goals the states that were reached in future time steps along the same trajectory as s_t [50]. As we want to sample states that are reached after executing a plan, we assume an arbitrary window size k . Concretely, to sample goals for a transition at time step t , we sample a discrete-time offset $\Delta \sim \text{Geom}(p)$, with $p \in [0, 1]$, and use the state at time $t + \Delta * (k - 1)$ as the goal. Note that if we assume consistent transitions from latent plan decoding, then if $\Delta = 1$, the reward for this transition is 1, as the low-level policy will reach the specified state after executing the plan, avoiding the sparsity issue.

However, relabeling all transitions in this manner introduces a problem: because the distance function is only trained on goals that have been achieved, it will systematically underestimate the distance to unreachable goals. We require a method for selecting “negative” goals that are distant, but still relevant. Randomly selecting states will produce pairs of images that are likely to be distant, but not necessarily relevant (e.g., pairs in which all objects and the robot have been moved). We want a goal sampling procedure that generates less obvious examples of distant states that are more informative. Similar to Tian et al. [51], we sample negative goal states s_g which have a similar proprioceptive state. This constraint enables the Q-function to learn to focus on the scene’s under-actuated parts (e.g., objects), which are likely to have distinct positions. As a result, these timesteps act as hard negatives, encouraging the model to pay closer attention to the scene. This sampling approach is computationally inexpensive, as we can query a precomputed k-nearest neighbors structure.

5 Experimental Results

We evaluate TACO-RL for learning a general-purpose robot in both simulated and real-world environments. The goals of these experiments are to investigate: (i) whether our hierarchical model is effective in performing complex long-horizon skills, (ii) how TACO-RL compares with alternative goal-conditioned policies, (iii) if our model scales to be used in real-world robotics.

5.1 Experimental Setup

We evaluate our approach in both simulated and real-world environments. We first investigate learning 7-DoF visuomotor robot skills in the CALVIN environment [16]. We train on the environment D of CALVIN, which contains 6 hours of unstructured play data collected via teleoperating a Franka Emika Panda robot arm to manipulate objects in a 3D tabletop environment.

Baselines Methods. As we aim to combine the complementary strengths of both paradigms, imitation and offline RL, we compare TACO-RL to representatives of the two extrema of the spectrum: the offline RL method *Conservative Q-learning* [6] extended by hindsight relabeling (CQL+HER) and the imitation learning method *Play-supervised Latent Motor Plan* (LMP) [13]. CQL+HER is trained on the derived reward as explained in Section 4.2 and introduces a penalty for out-of-distribution actions to limit the respective values of unseen actions. To make a fair comparison, this baseline is also trained with the negative mining trick. LMP, on the other hand, trains a goal conditioned imitation agent and resembles the low-level policy in TACO-RL, however, without any long-term optimality guarantees which TACO-RL accounts for by offline RL of a higher-level plan-selective policy. Additionally, we also compare against *Relay Imitation Learning* (RIL) [32]. This algorithm is the most related hierarchical algorithm, as it also learns from offline play data. RIL represents the family of methods that learns to predict latent subgoals for a low level policy.

5.2 Simulation Results

We start by evaluating our approach in the CALVIN environment [16]. This is a challenging environment as the scene changes through time and we act by using only RGB images of a static camera as input. As there is no predefined reward signal in this dataset, we relabel the transitions analogously as we do with TACO-RL. We investigate if our method is capable of performing complex long-horizon tasks in a robot control setting. We first attempt to solve 500 unique chains of 5 image-based goals queried in a row. For each subtask in a row the policy is conditioned on the current sub-goal image instruction and transitions to the next sub-goal only if the agent successfully completes the current task or if 180 timesteps have passed without reaching a success. We call this evaluation of performing multiple tasks on a row, long-horizon multitask with visual observations *LH-MTVis*. This setting is very challenging as it requires agents to be able to transition between different subgoals. Additionally, we ablate our model by increasing the negative goals ratio to 50% and removing the negative mining.

Method	LH-MTVis					
	No. Instructions in a Row (500 chains)					
	1	2	3	4	5	Avg. Len.
Ours	95.4% ±2	82% ±7.3	57.8% ±15	32.7% ±10	6.9% ±3.1	2.7 ±0.3
No neg. goals	94.9% ±4.5	69.7% ±14.3	31.1% ±15.7	5.5% ±4.5	0.9% ±0.8	2.02 ±0.4
50% neg. goals	71.8% ±2.2	27.1% ±1.8	6.2% ±2.6	0.2% ±0.3	0% ±0	1.05 ±0.1
RIL [32]	70.3% ±3.5	32.9% ±7.2	10.5 ±4.01	2.4 ±0.7	0.1 ±0.1	1.17 ±0.15
LMP [13]	91.4% ±2.3	63.3% ±3.5	23.1% ±2.2	3.6% ±0.9	0.2% ±0.08	1.8 ±0.08
CQL+HER	65.5% ±12.7	25.3% ±11	5.6% ±3.2	0.6% ±0.2	0%	0.9 ±0.2

Table 1. Success rates of models running 500 chains per three different random seeds, using intermediate sub-goal images.

In Table 1. we can see that TACO-RL is able to outperform all baselines. This experiment demonstrates that our agent is able to transition between different sub-goal images more naturally, enabling chaining more tasks in a row. Through our ablations, we observe that the performance of our model drops significantly when increasing the negative goal ratio to 50%. This result is to be expected as reducing the number of positive examples leads to a less informative reward indicating which are the useful behaviors to reach a transition. If we remove the negative goals from the goal distribution, the agent is still able to perform more sequential tasks than the baselines, but it underestimates the distance to the goals. This results in a decreased performance compared to our full approach.



Figure 4. **Real-world Manipulation Tasks.** Examples shown from left to right are: closing the drawer, opening the drawer, moving the sliding door left, moving the sliding door right, lifting the block, rotating the block, pushing the block, turning the green LED on, placing the block on top of the drawer and placing the block in the container.

We then evaluate the capacity of our model to perform 1000 rollouts of two sequential tasks using a single goal image. For this, we allow the agent to perform actions until 300 timesteps has passed. We record the success rate of all models in Table 2. TACO-RL successfully performs long-horizon tasks that require reasoning over sequential behaviors with a final success rate of 27% which corresponds to an order of magnitude improvement upon the LMP and CQL+HER baselines. RIL also exploits a hierarchical structure which allows it to reason over longer horizons than the other baselines, but TACO-RL still obtains more than two times its accuracy when performing both sequential tasks using a single image, proving its effectiveness in chaining skills through dynamic programming.

We further test the capacity of the models to perform a single task when the goal image does not contain the robot performing the task, but the end effector appears in another position after the task was performed (cf. Table 3). We run 50 rollouts for each task. These harder tasks require reasoning about changes in the scene and additionally evaluates generalization, as each rollout uses a different goal image not seen during training. With our ablations, we can see that including the negative goals in our framework contributes greatly to obtain a good performance in this scenario alleviating to not only imitate the final end effector position, but to reach the entire scene configuration. We noticed that TACO-RL was able to outperform the baselines, which can be explained through the skill-chaining abilities of our model and the negative goal mining used to train the critic network of the high-level policy. On the other hand, CQL+HER is not able to achieve the desired goal image and LMP has a strong bias towards the end-effector position ignoring the changes in the environment. RIL can imagine intermediate latent sub-goals required to achieve the task, which reduces the bias towards the end effector position, but it stills obtain a lower accuracy rate than our method.

Method	LH-MTVis		
	No. Instructions in a Row (1000 chains)		
	1	2	Avg. Len.
Ours	67.9% ±3.9	27% ±2.5	0.94 ±0.06
No neg. goals	39.5%±2.7	4.2%±1.6	0.44±0.04
50% neg. goals	45.4%±5.2	6.3%±0.6	0.52±0.05
RIL [32]	66.2%±6.5	13.3%±2.3	0.79±0.09
LMP [13]	34.3%±3.2	2.7%±0.1	0.3±0.03
CQL+HER	35.2%±3.4	2.4%±0.8	0.37±0.04

Table 2. Success rates of models running 1000 chains per three different random seeds conditioned only on the last goal image.

Method \ Task	Place block in drawer	Open drawer	Move slider left	Turn on lightbulb
Ours	94% ±8.7	87.3% ±5	79.3% ±11.7	94% ±4
No neg. goals	77.3%±6.1	37.3%±32.3	13.3%±9.5	9.3%±6.1
50% neg. goals	88%±7.2	58.7%±21.6	39.3%±25.3	92%±4
RIL [32]	74.67%±26.6	87.3% ±1.15	77%±1.4	92.7%±2.3
LMP [13]	78.6%±6.1	12%±2	12%±5.2	10%±2
CQL+HER	67.6%±20.8	8.6%±5	17.3%±8	4%±4

Table 3. The average success rate of goal-conditioned models running 50 rollouts where the goal image does not contain the end effector performing the task. Three models trained from different random seeds were used to perform the rollouts.

5.3 Real-Robot Experiments

For the real-world experiments, we investigate learning a single policy capable of performing multiple goal conditioned tasks. Examples of the tasks are shown in Figure 4. To generate the training dataset we collected nine hours of play data recorded via teleoperating a Franka Emika Panda robot arm with a VR controller. To avoid self-occlusions in the scene, these models also receive RGB

images of a gripper camera as an additional input. After training the models with the offline dataset, we performed 20 rollouts for each task using multiple goal images and start positions. TACO-RL was able to outperform the baselines consistently, especially when evaluated from a start position far away from the goal image or that required extended reasoning. We recorded the success rate of each model in Table 4.

Task \ Method	Ours	LMP [13]	CQL+HER
Lift the block on top of the drawer	60%	60%	20%
Lift the block inside the drawer	65%	50%	15%
Lift the block from the slider	60%	30%	10%
Lift the block from the container	65%	60%	20%
Lift the block from the table	70%	70%	30%
Place the block on top of the drawer	60%	50%	30%
Place the block inside the drawer	70%	40%	20%
Place the block in the slider	30%	0%	0%
Place the block in the container	65%	30%	15%
Stack the blocks	30%	0%	0%
Unstack the blocks	30%	10%	0%
Rotate block left	70%	40%	10%
Rotate block right	70%	50%	15%
Push block left	60%	50%	20%
Push block right	60%	50%	10%
Close drawer	90%	70%	20%
Open drawer	70%	50%	10%
Move slider left	75%	30%	0%
Move slider right	70%	10%	0%
Turn red light on	60%	30%	0%
Turn red light off	50%	20%	0%
Turn green light on	70%	60%	10%
Turn green light off	65%	50%	10%
Turn blue light on	50%	50%	5%
Turn blue light off	50%	30%	10%
Average over tasks	61%	40%	11%

Table 4. The average success rate of the multi-task goal-conditioned models running roll-outs in the real world.

We also tested our approach to perform sequential tasks with the real robot to verify that our approach can be scaled for long-horizon tasks. For this experiment we use a goal image for each task that the robot executes. See the supplementary video for qualitative results that showcase the diversity of tasks and the long-horizon capabilities of the different methods. Our agent trained completely from unlabeled play data is able to successfully perform most of these sequential tasks, by inferring how to transition between tasks and reach the state depicted by the goal image. More details in Appendix F.3.

Finally, we evaluate TACO-RL performing complex tasks with a single goal image, such as lifting the block and moving it to a desired position, and stacking a block on top of another. These tasks requires the agent to reason in a long-horizon manner, as if the robot imitates only the end effector position, the objects would not be arranged correctly in the scene. By stitching together the learned latent behaviors, our model was able to perform these tasks consistently.

6 Conclusion and Limitations

In this paper, we introduced *Task-Agnostic Offline Reinforcement Learning* (TACO-RL), which exploits a latent plan representation estimated from unstructured play data to effectively limit the horizon of a high-level offline RL policy acting upon this latent plan space. By dividing sequential multi-tier tasks into chunks of implicit subtasks solved by imitation learning, TACO-RL showed up to an order-of-magnitude improvement in performance compared to state-of-the-art both imitation learning and offline reinforcement learning baselines in both, simulated and real robot control tasks.

While TACO-RL is quite capable, it does have a number of limitations. Specifying a task to the requires providing a suitable goal image at test-time, which should be consistent with the current scene. Besides, tracking task progress might be useful when sequencing skills of different time horizons. We discuss limitations in more detail in Appendix H. But overall, we are excited about the confluence of imitation and offline RL methods towards scaling robot learning.

Acknowledgments

This work has been supported partly by the German Federal Ministry of Education and Research under contract 01IS18040B-OML.

References

- [1] V. Mnih, K. Kavukcuoglu, D. Silver, A. A. Rusu, J. Veness, M. G. Bellemare, A. Graves, M. Riedmiller, A. K. Fidjeland, G. Ostrovski, et al. Human-level control through deep reinforcement learning. *Nature*, 518(7540):529–533, 2015.
- [2] D. Silver, T. Hubert, J. Schrittwieser, I. Antonoglou, M. Lai, A. Guez, M. Lanctot, L. Sifre, D. Kumaran, T. Graepel, et al. A general reinforcement learning algorithm that masters chess, shogi, and go through self-play. *Science*, 362(6419):1140–1144, 2018.
- [3] M. Riedmiller, R. Hafner, T. Lampe, M. Neunert, J. Degraeve, T. van de Wiele, V. Mnih, N. Heess, and J. T. Springenberg. Learning by playing solving sparse reward tasks from scratch. In J. Dy and A. Krause, editors, *Proceedings of the 35th International Conference on Machine Learning*, volume 80 of *Proceedings of Machine Learning Research*, pages 4344–4353. PMLR, 10–15 Jul 2018.
- [4] T. Haarnoja, S. Ha, A. Zhou, J. Tan, G. Tucker, and S. Levine. Learning to walk via deep reinforcement learning. In *Proceedings of Robotics: Science and Systems*, 2019.
- [5] S. Levine, A. Kumar, G. Tucker, and J. Fu. Offline reinforcement learning: Tutorial, review, and perspectives on open problems. *arXiv preprint arXiv:2005.01643*, 2020.
- [6] A. Kumar, A. Zhou, G. Tucker, and S. Levine. Conservative q-learning for offline reinforcement learning. *Advances in Neural Information Processing Systems*, 33:1179–1191, 2020.
- [7] S. Fujimoto, D. Meger, and D. Precup. Off-policy deep reinforcement learning without exploration. In *International Conference on Machine Learning*, pages 2052–2062. PMLR, 2019.
- [8] S. Fujimoto and S. Gu. A minimalist approach to offline reinforcement learning. In *Advances in Neural Information Processing Systems*, 2021.
- [9] T. Yu, G. Thomas, L. Yu, S. Ermon, J. Y. Zou, S. Levine, C. Finn, and T. Ma. Mopo: Model-based offline policy optimization. In *Advances in Neural Information Processing Systems*, volume 33, pages 14129–14142. Curran Associates, Inc., 2020.
- [10] I. Kostrikov, A. Nair, and S. Levine. Offline reinforcement learning with implicit q-learning. In *International Conference on Learning Representations*, 2022.
- [11] R. Kidambi, A. Rajeswaran, P. Netrapalli, and T. Joachims. Morel: Model-based offline reinforcement learning. In *NeurIPS*, 2020.
- [12] Y. Chebotar, K. Hausman, Y. Lu, T. Xiao, D. Kalashnikov, J. Varley, A. Irpan, B. Eysenbach, R. C. Julian, C. Finn, et al. Actionable models: Unsupervised offline reinforcement learning of robotic skills. In *International Conference on Machine Learning*, pages 1518–1528. PMLR, 2021.
- [13] C. Lynch, M. Khansari, T. Xiao, V. Kumar, J. Tompson, S. Levine, and P. Sermanet. Learning latent plans from play. In *Conference on robot learning*, pages 1113–1132. PMLR, 2020.
- [14] A. Kumar, J. Hong, A. Singh, and S. Levine. Should i run offline reinforcement learning or behavioral cloning? In *International Conference on Learning Representations*, 2022.
- [15] P. Florence, C. Lynch, A. Zeng, O. A. Ramirez, A. Wahid, L. Downs, A. Wong, J. Lee, I. Mordatch, and J. Tompson. Implicit behavioral cloning. In *Conference on Robot Learning*, 2021.
- [16] O. Mees, L. Hermann, E. Rosete-Beas, and W. Burgard. Calvin: A benchmark for language-conditioned policy learning for long-horizon robot manipulation tasks. *IEEE Robotics and Automation Letters (RA-L)*, 7(3):7327–7334, 2022.

- [17] I. Kostrikov, R. Fergus, J. Tompson, and O. Nachum. Offline reinforcement learning with fisher divergence critic regularization. In *ICML*, volume 139 of *Proceedings of Machine Learning Research*, pages 5774–5783. PMLR, 2021.
- [18] A. Gupta, C. Lynch, B. Kinman, G. Peake, S. Levine, and K. Hausman. Demonstration-bootstrapped autonomous practicing via multi-task reinforcement learning. *arXiv*, 2022.
- [19] X. B. Peng, M. Chang, G. Zhang, P. Abbeel, and S. Levine. Mcp: Learning composable hierarchical control with multiplicative compositional policies. *Advances in Neural Information Processing Systems*, 32, 2019.
- [20] P.-L. Bacon, J. Harb, and D. Precup. The option-critic architecture. In *Proceedings of the AAAI Conference on Artificial Intelligence*, volume 31, 2017.
- [21] O. Rybkin, C. Zhu, A. Nagabandi, K. Daniilidis, I. Mordatch, and S. Levine. Model-based reinforcement learning via latent-space collocation. In *ICML*, volume 139 of *Proceedings of Machine Learning Research*, pages 9190–9201. PMLR, 2021.
- [22] K. Pertsch, O. Rybkin, F. Ebert, S. Zhou, D. Jayaraman, C. Finn, and S. Levine. Long-horizon visual planning with goal-conditioned hierarchical predictors. In *NeurIPS*, 2020.
- [23] K. Pertsch, O. Rybkin, J. Yang, S. Zhou, K. G. Derpanis, K. Daniilidis, J. J. Lim, and A. Jaegle. Keyframing the future: Keyframe discovery for visual prediction and planning. In *LADC*, volume 120 of *Proceedings of Machine Learning Research*, pages 969–979. PMLR, 2020.
- [24] S. Nair and C. Finn. Hierarchical foresight: Self-supervised learning of long-horizon tasks via visual subgoal generation. In *International Conference on Learning Representations*, 2020.
- [25] D. Jayaraman, F. Ebert, A. A. Efros, and S. Levine. Time-agnostic prediction: Predicting predictable video frames. In *International Conference on Learning Representations*, 2019.
- [26] K. Fang, Y. Zhu, A. Garg, S. Savarese, and L. Fei-Fei. Dynamics learning with cascaded variational inference for multi-step manipulation. In *CoRL*, volume 100 of *Proceedings of Machine Learning Research*, pages 42–52. PMLR, 2019.
- [27] B. Ichter, P. Sermanet, and C. Lynch. Broadly-exploring, local-policy trees for long-horizon task planning. In *CoRL*, volume 164 of *Proceedings of Machine Learning Research*, pages 59–69. PMLR, 2021.
- [28] L. X. Shi, J. J. Lim, and Y. Lee. Skill-based model-based reinforcement learning. *arXiv preprint arXiv:2207.07560*, 2022.
- [29] K. Pertsch, Y. Lee, and J. J. Lim. Accelerating reinforcement learning with learned skill priors. In *CoRL*, volume 155 of *Proceedings of Machine Learning Research*, pages 188–204. PMLR, 2020.
- [30] K. Fang, P. Yin, A. Nair, and S. Levine. Planning to practice: Efficient online fine-tuning by composing goals in latent space. *arXiv preprint arXiv:2205.08129*, 2022.
- [31] S. Nasiriany, V. Pong, S. Lin, and S. Levine. Planning with goal-conditioned policies. In *NeurIPS*, pages 14814–14825, 2019.
- [32] A. Gupta, V. Kumar, C. Lynch, S. Levine, and K. Hausman. Relay policy learning: Solving long-horizon tasks via imitation and reinforcement learning. In *CoRL*, volume 100 of *Proceedings of Machine Learning Research*, pages 1025–1037. PMLR, 2019.
- [33] O. Nachum, S. Gu, H. Lee, and S. Levine. Data-efficient hierarchical reinforcement learning. In *NeurIPS*, pages 3307–3317, 2018.
- [34] T. Shankar and A. Gupta. Learning robot skills with temporal variational inference. In *International Conference on Machine Learning*, pages 8624–8633. PMLR, 2020.
- [35] J. Borja-Diaz, O. Mees, G. Kalweit, L. Hermann, J. Boedecker, and W. Burgard. Affordance learning from play for sample-efficient policy learning. In *ICRA*, Philadelphia, USA, 2022.

- [36] A. Mandlekar, D. Xu, R. Martín-Martín, S. Savarese, and L. Fei-Fei. GTI: learning to generalize across long-horizon tasks from human demonstrations. In *Robotics: Science and Systems*, 2020.
- [37] D. Xu, S. Nair, Y. Zhu, J. Gao, A. Garg, L. Fei-Fei, and S. Savarese. Neural task programming: Learning to generalize across hierarchical tasks. In *ICRA*, pages 1–8. IEEE, 2018.
- [38] D. Shah, P. Xu, Y. Lu, T. Xiao, A. T. Toshev, S. Levine, et al. Value function spaces: Skill-centric state abstractions for long-horizon reasoning. In *International Conference on Learning Representations*, 2021.
- [39] A. Singh, H. Liu, G. Zhou, A. Yu, N. Rhinehart, and S. Levine. Parrot: Data-driven behavioral priors for reinforcement learning. In *International Conference on Learning Representations*, 2021.
- [40] D. Ghosh, A. Gupta, and S. Levine. Learning actionable representations with goal conditioned policies. In *ICLR (Poster)*. OpenReview.net, 2019.
- [41] O. Nachum, M. Ahn, H. Ponte, S. S. Gu, and V. Kumar. Multi-agent manipulation via locomotion using hierarchical sim2real. In *Conference on Robot Learning*, pages 110–121. PMLR, 2020.
- [42] K. Hausman, J. T. Springenberg, Z. Wang, N. Heess, and M. Riedmiller. Learning an embedding space for transferable robot skills. In *International Conference on Learning Representations*, 2018.
- [43] O. Mees, M. Merklinger, G. Kalweit, and W. Burgard. Adversarial skill networks: Unsupervised robot skill learning from videos. In *ICRA*, Paris, France, 2020.
- [44] A. Ajay, A. Kumar, P. Agrawal, S. Levine, and O. Nachum. OPAL: offline primitive discovery for accelerating offline reinforcement learning. In *International Conference on Learning Representations*, 2021.
- [45] L. Wang, X. Meng, Y. Xiang, and D. Fox. Hierarchical policies for cluttered-scene grasping with latent plans. *IEEE Robotics and Automation Letters*, 2022.
- [46] D. P. Kingma and M. Welling. Auto-encoding variational bayes. *arXiv preprint arXiv:1312.6114*, 2013.
- [47] I. Higgins, L. Matthey, A. Pal, C. P. Burgess, X. Glorot, M. M. Botvinick, S. Mohamed, and A. Lerchner. beta-vae: Learning basic visual concepts with a constrained variational framework. In *International Conference on Learning Representations*, 2017.
- [48] D. Hafner, T. P. Lillicrap, M. Norouzi, and J. Ba. Mastering atari with discrete world models. In *International Conference on Learning Representations*, 2020.
- [49] O. Mees, L. Hermann, and W. Burgard. What matters in language conditioned robotic imitation learning over unstructured data. *IEEE Robotics and Automation Letters (RA-L)*, 7(4):11205–11212, 2022.
- [50] M. Andrychowicz, F. Wolski, A. Ray, J. Schneider, R. Fong, P. Welinder, B. McGrew, J. Tobin, O. Pieter Abbeel, and W. Zaremba. Hindsight experience replay. *Advances in neural information processing systems*, 30, 2017.
- [51] S. Tian, S. Nair, F. Ebert, S. Dasari, B. Eysenbach, C. Finn, and S. Levine. Model-based visual planning with self-supervised functional distances. In *International Conference on Learning Representations*, 2021.
- [52] T. Salimans, A. Karpathy, X. Chen, and D. P. Kingma. Pixelcnn++: Improving the pixelcnn with discretized logistic mixture likelihood and other modifications. *arXiv preprint arXiv:1701.05517*, 2017.
- [53] S. Nair, A. Rajeswaran, V. Kumar, C. Finn, and A. Gupta. R3m: A universal visual representation for robot manipulation. *arXiv preprint arXiv:2203.12601*, 2022.

- [54] J. Fu, A. Kumar, O. Nachum, G. Tucker, and S. Levine. D4rl: Datasets for deep data-driven reinforcement learning. *arXiv preprint arXiv:2004.07219*, 2020.
- [55] O. Mees and W. Burgard. Composing pick-and-place tasks by grounding language. In *Proceedings of the International Symposium on Experimental Robotics (ISER)*, La Valletta, Malta, 2021.

Appendix

A Teleoperation Interface

A.1 Simulation

To collect data for simulation the human teleoperator uses the HTC VIVE Pro headset to visualize the CALVIN environment and its controller to collect play data. Clicking the application menu button emits a signal to start recording a play data episode, since then the robot arm tracks the controller’s position and orientation and maps it to the gripper end effector position and orientation.

Control	Function
Application menu	Starts or finishes recording a play data episode
Trigger	When pressed it closes the gripper end effector, otherwise it opens

A.2 Real World

For the real world we use the HTC VIVE Pro controller. At the beginning of the teleoperation, we calibrate our X axis position by clicking the grip button and moving towards its positive axis, we then click the application menu to indicate that we finished the calibration movement. This calibration procedure allows us to define the reference frame in which the global coordinates from the robot end effector is be recorded. In this setting, the teleoperator is facing the table in the same direction as the robot, hence if the controller moves right so does the robot. This way we can map the position of the controller to an absolute action defining the desired robot arm end effector 3D position. Additionally, we must press continuously the grip button to enable movement of the robot arm, this is to avoid involuntary hand tracking and prevent possible accidents.

Control	Function
Grip	Starts calibration; enables robot movement
Application menu	Finishes calibration; Starts or finishes recording a play data episode
Trigger	When pressed it closes the gripper end effector, otherwise it opens

B Experimental Setup Details

For both our real and simulated robot environments we use the following 7-dimensional action scheme:

$$[\delta x, \delta y, \delta z, \delta alpha, \delta beta, \delta gamma, gripper Action]$$

The $\delta x, \delta y, \delta z$ action dimensions corresponds to a change in the end effector’s position in 3D space. The $\delta alpha, \delta beta, \delta gamma$ action dimensions specifies a change in the end-effector’s orientation in the robot’s base frame. All these 6 dimensions accept continuous values between $[-1, 1]$. Finally, the *gripper Action* command can have two discrete values -1.0 and 1.0 . An action of -1.0 in this dimension commands the robot to open the gripper and 1.0 indicates that we desire to close it.

B.1 Data Collection Details

For the real world robot, we collected nine hours of play data by teleoperating a Franka Emika Panda robot arm, were we also manipulate objects in a 3D tabletop environment. This environment consists of a table with a drawer that can be opened and closed. The environment also contains a sliding door on top of a wooden base, such that the handle can be reached by the end effector. On top of the drawer, there are three led buttons with green, blue and orange coatings to be able to identify them, on the recorded play data we only interacted with the led button with green coating. When the led button is clicked, it toggles the state of the light. Additionally, there are three different colored blocks with letters on top. We visualize the data collection and setup in Figure 5.

In every time step we record the measurements from the robot proprioceptive sensors, as well as an static RGB-D image of size 150×200 from the Azure Kinect camera and a gripper RGB-D image of size 200×200 emitted by the FRAMOS Industrial Depth Camera D435e and the commanded absolute action. For this project we only use the static RGB image and the gripper camera RGB image as part of the observation. We visualize the input observations in Figure 6.

We extract the relative action a_t from the change in the absolute actions from time steps a_t and a_{t-1} as in practice, reproducing the relative actions computed this way showed a better performance than



Figure 5. Visualization of the real world data collection procedure (left) and the full robot setup (right).

when computed from the noisy measurements of the proprioceptive sensors. The data is collected at 30 Hz, but given that there is relatively a very small change in the end effector position between frames, we downsample the processed data to a frequency of 15 Hz.



Figure 6. Visualization of the observations obtained in the real world environment. On the left we show the RGB image captured by the static camera. On the right we show the RGB image captured by the gripper camera.

C Network Architecture

C.1 Hyperparameters for TACO-RL

Low-Level Policy: To learn the low-level policy we trained the model using 8 gpus with Distributed Data Parallel. Throughout training, we randomly sample windows between length 8 and 16 and pad them until reaching the max length of 16 by repeating the last observation and an action equivalent to keeping the end effector in the same state. We visualize the low-level policy architecture in Figure 7. Additional hyperparameters are listed below:

- Batch size of 64
- Latent plan dim of 16
- Learning rate of $1e - 4$
- The KL loss weight β is $1e - 3$ and uses KL balancing

These hyperparameters were chosen in order to make the action space of the high-level policy tractable for reinforcement learning, as the latent plan z is used as an action when learning the high-level policy.

High-Level Policy: Similarly as in the low-level policy, we also trained the model using 8 gpus with Distributed Data Parallel. We visualize the architecture in Figure 8. We use the following hyperparameters:

- Batch size of 64
- Learning rates – Q-function: $3e - 4$, Policy: $1e - 4$,
- Target network update rate of 0.005
- Ratio of policy to Q-function updates of 1 : 1
- Number of Q-functions: 2 Q-functions, $\min(Q1, Q2)$ used for Q-function backup and policy update

- Automatic entropy tuning: *True*, with target entropy set to $-\log |A|$
- CQL version: $CQL(\mathcal{H})$ (Using deterministic backup)
- α in CQL: 1.0 (we used the non-Lagrange version of $CQL(\mathcal{H})$)
- Number of negative samples used for estimating *logsumexp*: 4
- Initial BC warmstart epochs: 5
- Discount factor of 0.95

It is important to mention that the model performance is robust to slight changes in the hyperparameter selection.

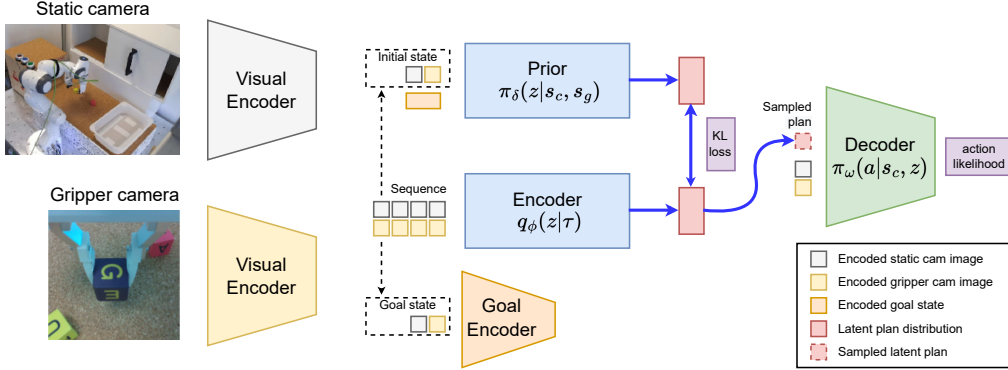


Figure 7. Overview of the architecture used in the real world to learn the low-level policy.

Goal Sampling Strategy: We use the same geometric distribution probability of $p = 0.3$ for all experiments. When this hyperparameter is closer to 0 it will be able to stitch plans to achieve longer horizon tasks, but it will encounter less often a reward of 1 which makes the optimization problem harder. For the 3D tabletop environment in both simulation and real world, we sample positive examples (goals from the future) 90% of the time and negative examples (goals with similar proprioceptive state) 10% of the time.

C.2 Encoder

The encoder (aka Posterior) $q_\phi(z|\tau)$ encodes the trajectory τ of state-action pairs into a distribution in latent space and gives out parameters of that distribution. In our case, we represent $q_\phi(z|\tau)$ with a transformer network, which takes τ and outputs parameters of a Gaussian distribution $(\mu_z^{enc}, \sigma_z^{enc})$. We encode the sequence of visual observations with our vision encoder. Then, we add positional embeddings to enable the experience window to carry temporal information. Finally, we fed the result into the transformer to learn temporally contextualized global video representations. In particular, our transformer encoder architecture consists of 2 blocks, 8 self-attention heads, and a hidden dimension of 2048.

C.3 Decoder

The decoder (aka Low-Level Policy): $\pi_\omega(a|s_c, z)$ is the latent-conditioned policy. It maximizes the conditional log-likelihood of actions in τ given the state and the latent vector. In our implementation, we parameterize it as a recurrent neural network which takes as input the current state and the sampled latent plan and gives out parameters of a discretized logistic mixture distribution [52]. For our experiments, we use 2 RNN layers each containing a hidden dimension of 2048. In the discretized logistic mixture distribution we use 10 distributions, predicting 10 classes per dimension. We predict an action where the 6 first dimensions are continuous in a range between -1.0 and 1.0 and its last dimension contains the gripper action, which is a discrete value optimized by cross entropy loss.

C.4 Prior

The prior $\pi_\delta(z|s_c, s_g)$ tries to predict the encoded distribution of the trajectory τ from its initial state and its goal state. Our implementation uses a feed-forward neural network which takes in the embedded representation of the initial state and goal state and predicts the parameters of a Gaussian distribution $(\mu_z^{pr}, \sigma_z^{pr})$. The prior network consists of 3 fully connected layers with a size of 256.

C.5 Visual Encoder

To obtain the current state embedded representation we pass each input modality observation through a convolutional encoder and we perform late fusion by concatenating the embedded representations of all the observation modalities.

Simulation

In simulation we only use the RGB static image as input, this is passed through the same convolutional encoder proposed in the original Play LMP implementation with 3 convolutional layers and a spatial softmax layer, after flattening its representation it is fed through two fully connected layers which output an embedded latent size of 32.

Real World

For the real world we use both RGB static image and the RGB gripper image as input. We send the RGB gripper image to a convolutional encoder as in original Play LMP implementation, with an embedded latent size of 32. For the RGB static image we used the pretrained R3M [53] Resnet18 networks with fixed weights, afterwards we passed it through 2 feedforward networks with a hidden size of 256 and an embedded latent size of 32.

C.6 Goal Encoder

We obtain a compact perceptual representation from the goal observation by passing it through the visual encoder. Then, we use 2 hidden layers with a size of 256 and an output layer that maps its representation to 32 latent features.

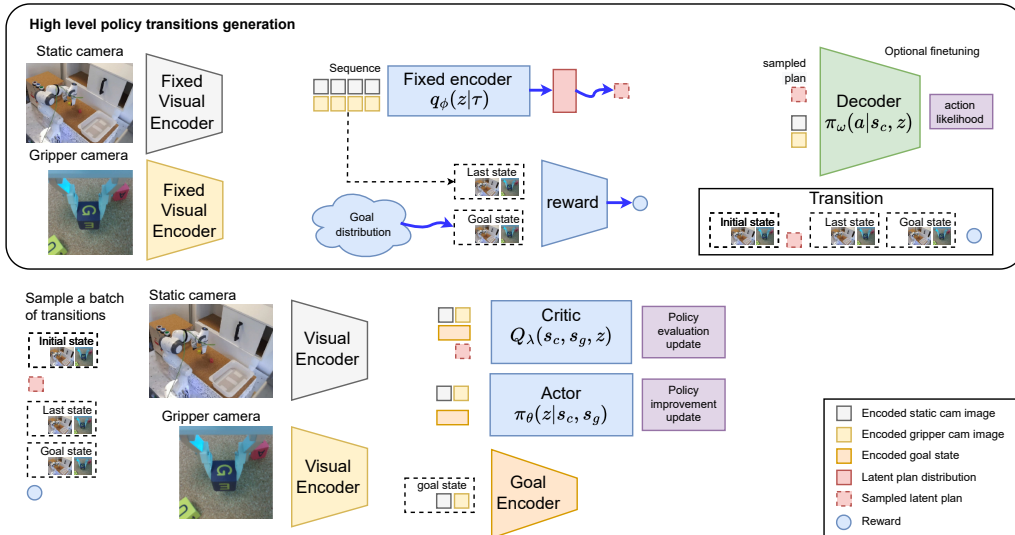


Figure 8. Overview of the architecture used in the real world to learn the high-level policy. We first used the learned low level policy to generate transitions using latent plans, afterwards we sample a batch of transitions and use CQL to learn the high level policy.

C.7 Actor

To learn the high level policy we use CQL. In particular, The actor network uses the same network architecture as the prior $\pi_\delta(z|s_c, s_g)$, as we can use the pre-learned weights as a good initialization. It has 3 hidden fully connected layers with a size of 256 and an output layer that predicts the mean and standard deviation of a latent plan Gaussian distribution.

C.8 Critic

The critic network takes as input the embedded representation of the current state, the encoded goal state and a sampled latent plan. All the inputs are concatenated and passed through a feed forward network with 3 hidden layers with a size of 256 and an output layer which predicts the expected state-action value of the policy.

D Policy Training Details

In this section we specify some implementation details of our baseline models used as comparison against TACO-RL.

D.1 Play-supervised Latent Motor Plans (LMP)

For our reimplementation of LMP we used the same network architecture described in C, the main differences with the original implementation is that the latent goal representation is only added to the prior, but not to the decoder. Additionally, we apply a tanh transformation to the sampled latent plan to ensure that every dimension is between -1.0 and 1.0 . Another difference with respect to the original formulation is that we implement a KL balancing. As the KL-loss is bidirectional, we want to avoid regularizing the plans generated by the posterior toward a poorly trained prior. To solve this problem, we minimize the KL-loss faster with respect to the prior than the posterior by using different learning rates, $\alpha = 0.8$ for the prior and $1 - \alpha$ for the posterior, similar to Hafner *et al.* [48]. These architectural changes were made to do a fair comparison against our implementation, and to make sure the improvements of our method were due to the plan stitching capabilities and our self-supervised reward function.

Additionally, the decoder predicts relative actions instead of absolute actions as this leads to an overall better performance. We note that our LMP baseline is implemented in the same way.

D.2 Conservative Q-Learning with Hindsight Experience Replay (CQL + HER)

We use the same visual encoder architecture as in TACO-RL. The critic networks are made with 3 fully connected layers using a hidden dimension of 256. The actor network also uses 3 fully connected layers with a size of 256 and predicts in the last dimension a discrete action to open and close the parallel gripper. This last dimension is predicted through a Gumbel Softmax distribution.

The self-supervised reward function is done similarly as in our method with a small difference when sampling goal states from the future. The CQL transitions are (s_t, a, s_{t+1}) instead of (s_t, z_t, s_{t+k-1}) , therefore when we sample a goal from discrete-time offset $\Delta \sim Geom(p)$, we use the observations at the time step $t + \Delta$ as a goal instead of the observation at the timestep $t + \Delta * (k - 1)$, where k is the window size and p is the same value for both implementations. This change is required as CQL needs to take isolated decisions every time step. In contrast, our formulation allows TACO-RL to reduce the effective episode horizon by predicting high-level actions (latent plans).

D.3 Relay Imitation Learning (RIL)

We use the same visual encoder architecture as in TACO-RL to do a fair comparison. For the policy architecture, we first tried the architecture proposed by the original authors of each policy using two layer neural networks with 256 units each and ReLU nonlinearities. This architecture obtained poor performance for our application, we noticed that the respective loss objectives were not being correctly optimized for which we solved this issue by training a bigger network. For our tested implementation, for both the high-level and low-level policy we used four layer neural networks with 1024 units each.

E Data Preprocessing

E.1 Simulation

In simulation we only use the static camera RGB image as input, we first resize the RGB image from 200×200 to 128×128 . Then we perform stochastic image shifts of $0 - 6$ pixels to the static camera images and a bilinear interpolation is applied on top of the shifted image by replacing each pixel with the average of the nearest pixels. Then we apply a color jitter transform augmentation with a contrast of 0.1, a brightness of 0.1 and hue of 0.02. Finally, we normalize the input image to have pixels with float values between -1.0 and 1.0 .

E.2 Real World

In the real world as there are several occlusions only using the static camera RGB image, we also add the gripper camera RGB image to the observation. For the static camera RGB image we use the original size of 150×200 , we then apply a color jitter transform with contrast of 0.05, a brightness of 0.05 and a hue of 0.02. Finally, we use the values for the pretrained R3M normalization, i.e., mean = $[0.485, 0.456, 0.406]$ and a standard deviation, std = $[0.229, 0.224, 0.225]$.

For the gripper camera RGB image we resize the image from 200×200 to 84×84 , we then apply a color jitter transform with contrast of 0.05, a brightness of 0.05 and a hue of 0.02. Then we perform stochastic image shifts of $0 - 4$ pixels to the and a bilinear interpolation is applied on top of the shifted image by replacing each pixel with the average of the nearest pixels. Finally, we normalize the input image to have pixels with float values between -1.0 and 1.0 .

F Additional Results

F.1 CALVIN

We add the rest of the results of all the different tasks that could be made in the CALVIN environment where the goal image does not need to contain the robot end effector performing the task in Figure 9. We run 50 rollouts for each task. Each rollout uses a different goal image which was not seen throughout training.

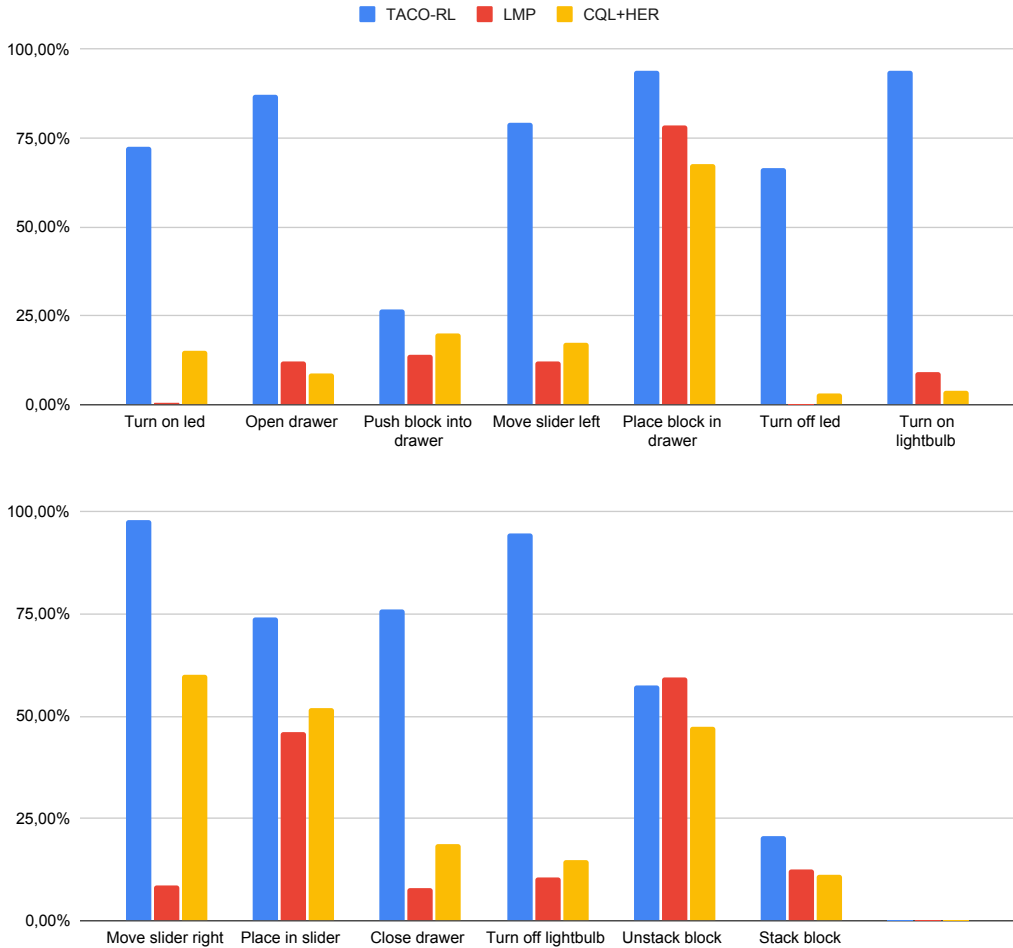


Figure 9. The average success rate of goal-conditioned models running 50 rollouts where the goal image does not contain the end effector performing the task. Results were calculated using 3 seeds.

F.2 Maze2D

We also evaluate our algorithm in the Maze2D environments from D4RL [54]. These tasks are designed to provide a simple test that the model is capable of stitching together various subtrajectories such that the agent is capable of reaching the goal in the smallest amount of steps. For TACO-RL, we learn the policy by relabeling the transitions instead of using the rewards given by the dataset. Additionally, given that the scene does not change through time, we only add positive examples in our goal sampling approach. We perform the rollouts of both LMP and TACO-RL by exposing the desired target position. TACO-RL outperforms both LMP and CQL as it is able to stitch plans through dynamic programming as shown in Table 5.

F.3 Real World

To make sure that our method can be scaled for long-term tasks, we used our framework to control a real robot to carry out consecutive tasks. For the purposes of this experiment, we assign a goal

Environment	TACO-RL	LMP [13]	CQL [6]
maze2d-umaze	110 \pm 2.2	81.9 \pm 14.9	5.7
maze2d-medium	88.9 \pm 2	77 \pm 18	5.0
maze2d-large	76.7 \pm 9.7	20.1 \pm 29.3	12.5

Table 5. The average normalized score for three different random seeds. The CQL results were obtained from the D4RL whitepaper [54].

image for each of the robot’s tasks. Our agent, which was trained entirely from unlabeled play data, can complete all of these sequential tasks by inferring how to transition between them, achieving the state depicted by the goal image. Examples of these sequential tasks are listed below:

- Moving the sliding door to the right and then opening the drawer
- Lifting the block and putting it on top of the drawer
- Lifting the block and placing it on a plastic container
- Turning the blue light on and then opening the drawer
- Turning the green light on and then open the drawer

G Negative Results

We present an incomplete list of experiments tried throughout the course of the research project. These ideas were tried a couple of times, but they in general do not improve performance. It is possible that they could work better with a more thorough investigation. We hope this experience will be helpful to researchers building on top of this work.

- Predicting absolute actions instead of relative actions with the decoder decreases the low-level policy performance. We believe that using relative actions might be easier for the agent to learn, as it does not have to memorize all the locations where an interaction has been performed.
- Decoder designed only with fully connected layers instead of a recurrent neural network lead to a slightly worse performance. We speculate that this could be due to the environment not completely following the Markov assumption.
- Using a gaussian mixture model instead of a mixture of logistics to predict the decoder actions lead to a similar performance.
- Using a pretrained ResNet18 in the imagenet dataset as visual encoder in simulation decreases performance for the low-level policy. More experiments by using the R3M pretrained model in simulation might offer different results.
- In the real world experiments, training the visual encoder from scratch for the static camera network decreases performance for the low-level policy. This can be explained due to the small amount of data present in the real-world dataset.

H Limitations

Despite the promising ability to learn diverse goal-reaching tasks even reasoning over long-horizon tasks, our method has a few aspects that warrant future research. Specifying a task to the goal-conditioned policy, requires providing a suitable goal image at test-time, which should be consistent with the current scene. An exciting direction for future work is to use natural language processing techniques to command the robot policy [55, 49]. If one wishes to sequence various tasks in the real world, an open question we did not address in this work is tracking task progress, in order to know when to move to the next task. In this work we acted with a fixed time-horizon for sequencing tasks in the real world, but this implicitly assumes that all tasks take approximately the same timesteps to complete. In addition, recent results [14] show that, in general, pure offline RL methods tend to offer better data-efficiency compared to behavioral cloning, which could be counted as one general limitation of imitation learning methods and derivatives of it, as the approach introduced in this work. However, since one of the most appealing properties of play lies in the simplicity of data collection, this limitation appears to be rather minor. Our method has a specific limitation in that we must first train the low-level policy before training the high-level policy, which requires more training time than training them together. However, because we train our approach offline, the robot does not need to perform rollouts in the environment during this time, making this a minor issue.